Proceedings of the 6th International Conference on Biological Engineering and Medical Science
DOI: 10.54254/2753-8818/2026.36819

Reaction-Induced Modulation Strategies in Bisulfite-Responsive Fluorescent Probes

Zhengyang Guo

Department of Science, Dalhousie University, Halifax, Canada
zh249112@dal.ca

Abstract. Sulfur dioxide (SO_2), a major air pollutant, causes serious environmental impacts such as acid rain. In addition, the human body generates endogenous SO_2, which functions as a gasotransmitter to regulate physiological systems and inflammatory pathways. Congenital disorders, including molybdenum cofactor deficiency (MoCD) and sulfite oxidase deficiency, lead to sulfite imbalance and severe developmental impairments of the nervous system. Therefore, accurate analysis of both endogenous and exogenous SO_2 levels is crucial. Fluorescence probes have emerged as an alternative approach for sulfite detection. Compared with traditional methods, they offer unique advantages such as rapid response, high sensitivity, high selectivity, and non-invasive, real-time imaging in biological samples. These probes typically rely on chemical reactions (e.g., Michael addition, aldehyde addition, levulinate deprotection) with sulfite, which induce structural changes in the probe and subsequently activate or suppress photophysical pathways. As a result, changes in fluorescence intensity or wavelength can be observed. Nevertheless, challenges remain in both in vivo and in vitro sulfite analysis. Effective probes often require bulky or hydrophobic structures to penetrate cell membranes, and their potential toxicity must also be carefully evaluated.

Keywords: fluorescent probe, sulfite, bisulfite, reaction mechanism, photophysical processes

1. Introduction

Sulfur dioxide (SO_2) has been recognized as one of the "six criteria air pollutants" due to its significant environmental impacts [1]. In the atmosphere, SO_2 can be oxidized to sulfuric acid and sulfate aerosols [1]. Beyond its environmental role, SO_2 can also be endogenously produced in animals, where it is regarded as a gasotransmitter involved in the regulation of physiological processes [1, 2].

Physiological SO_2 contribute to lowering blood pressure, maintaining vascular integrity, reducing myocardial and pulmonary injury, preventing myocardial hypertrophy, and protecting neuronal function [2]. In contrast, excessive SO_2 exposure induces oxidative stress and macromolecular damage to proteins, lipids, and DNA, leading to multi-system toxicity and a high carcinogenic risk [2]. Metabolic imbalance is further associate with genetic disorder such as molybdenum cofactor deficiency (MoCD) and sulfite oxidase (SO) deficiency. They commonly disrupt sulfite metabolism and result in impair the oxidation of endogenous sulfite (SO_3^{2-}) to sulfate (SO_4^{2-}) due to defects in

© 2026 The Authors. This is an open access article distributed under the terms of the Creative Commons Attribution License 4.0 (https://creativecommons.org/licenses/by/4.0/).

DOI: 10.54254/2753-8818/2026.36819

Moco biosynthesis or deterioration of SO activity, respectively [3, 4]. These congenital deficiencies rapidly trigger severe neonatal neurotoxicity, typically showing in neurological abnormalities, seizures, and dysmorphic features [3, 4].

Therefore, accurate quantification of endogenous sulfite is essential. Traditional methods (titration, flow injection analysis, capillary electrophoresis, HPLC) rely on harsh reagents (e.g., strong oxidants, acids) and complex sample preparation [5]. Thus, these characteristics limiting their usage to food and environmental analysis rather than real-time biological detection [5]. Instead, various reaction and photophysical mechanisms have been adapted in fluorescence probes as alternative approach for sulfite detection. They have unique benefits in rapid response, high sensitivity, and exceptional selectivity. They also enable real-time non-invasive visualization of HSO_3^-/SO_3^{2-} in vivo and in vitro. Therefore, this review highlights their design strategies and applications with the propose of providing a clear overview of fluorescence probes in sulfite detection.

2. Fluorescent probes as alternative detection approach for bisulfite

Sulfite-detecting fluorescence probes are designed based on the strong nucleophilicity of HSO_3^-/SO_3^{2-}. Probes usually react with electron-deficient sites in the molecule to cause changes in fluorescence emission. Their fluorescence phenomena are commonly triggered by α,β-unsaturated bond (Michael addition), an aldehyde group (nucleophilic addition), or a levulinate ester (deprotection) [6]. Combined with changes in photophysical processes, such as Intramolecular Charge Transfer (ICT) [7-9], Twisted Intramolecular Charge Transfer (TICT) [10], Aggregation-Induced Emission (AIE) [11], Förster Resonance Energy Transfer (FRET) [9, 12], or Excited-State Intramolecular Proton Transfer (ESIPT) [7, 9].As a result of fluorescence emission change models of turn-on, turn-off, or ratiometric response for quantitative analysis and bioimaging. Furthermore, dual-channel response and logic gate model probes strategies enable complex signal outputs, provide the possibility of multi-target detection. In this section, fluorescence probes are summarized according to reaction mechanisms and their photophysical processes are highlighted.

2.1. Fluorescence probes based on michael addition reaction

The most widely employed mechanism in sulfite-responsive fluorescent probes is Michael addition, where HSO_3^- nucleophilic attacks an electron-deficient C=C double bond of the probe. This reaction disrupts the donor-π-acceptor (D-π-A) conjugation system, thereby altering the photophysical properties of the fluorophore [6]. Based on this principle, numerous small-molecule probes have been developed for the detection and imaging of sulfur derivatives.

2.1.1. ICT-modulated probes

Intramolecular Charge Transfer (ICT) occurs in donor-π-acceptor (D-π-A) systems [7-9]. The π-conjugated bridge provides an electron transfer channel between the donor (D) and acceptor (A), forming a push-pull structure [8]. Upon photoexcitation, electron density shifts from the donor to acceptor, producing characteristic fluorescence emission [7, 8]. When sulfite undergoes nucleophilic addition at the C=C bond of the probe, the π-conjugation is disrupted, attenuating or restoring ICT. Thereby changes in fluorescence intensity and/or emission wavelength are observed [7-9].

Luo et al. (2025) developed a Michael addition and ICT process-based probe [13], DCM-MQE, a dicyanomethylene-4*H*-pyran derivative with a methylquinolinium acceptor. Upon nucleophilic

DOI: 10.54254/2753-8818/2026.36819

addition of sulfite to the C=C bond, the quinolinium unit is converted into an electron-rich enamine, thereby activating ICT and producing a turn-on fluorescence at 661 nm (Figure 1) [13].

Based on Michael addition and ICT processes, Ji and co-workers [14] designed two probes, DPQ-1 and DPQ-2, derived from quinoline-nitrile and pyran-nitrile scaffolds. In these systems, the methylquinolinium unit is conjugated to the acceptors via a C=C bond. Upon nucleophilic addition of HSO_3^- to this electron-deficient site, the quinolinium moiety is converted into an electron-donating enamine, thereby activating the ICT pathway and producing enhanced fluorescence (Figure 1). The reaction transforms the electronic configuration from A-π-A to D-π-A in DPQ-1, and from A-A-A to D-A-D in DPQ-2, resulting in turn-on emissions at 590 nm and 600 nm, respectively (Figure 1) [14].

Yan et al. [15] reported MDQ, a dicyanoisophorone-methylquinolinium conjugate designed for sulfite detection. Through Michael addition of SO_3^{2-}, the probe restores the ICT pathway and generates a strong NIR emission at 670 nm (Figure 1) [15].

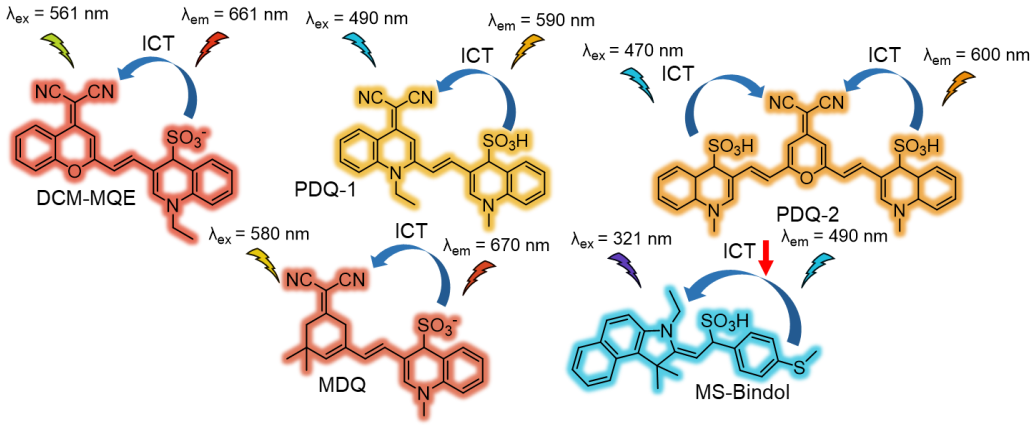

Figure 1. Representative post-reaction structures of Michael addition probes based on ICT [13, 16]

Zhang et al. [16] developed MS-Bindol, a hemicyanine probe incorporating a C=C bond as the recognition site. Upon Michael addition of SO_2 derivatives, the ICT pathway is suppressed, resulting in a fluorescence turn-on at 490 nm (Figure 1) [16].

2.1.2. AIE-characteristic probes

Aggregation-Induced Emission (AIE) describes fluorophores that are weakly emissive in dilute solution but become strongly fluorescent upon aggregation, due to restriction of intramolecular motion (RIM) [11]. AIEgens in probes typically show enhanced emission upon aggregation. Michael addition alters molecular rigidity or conjugation, thereby modulating AIE fluorescence, resulting in either turn-on, ratiometric shifts, or quenching [17-19]. AIE-based probes deliver high signal-to-noise ratios, outstanding photostability, and are ideal for wash-free imaging and on-site detection.

Diwan et al. [17] developed R1, a pyrene-benzthiazolium conjugate probe that combines Michael addition, AIE, and ICT processes. In aqueous solution, the planar conformation of R1 promotes J-aggregation, restricting intramolecular rotation (RIR) and enhancing fluorescence (Figure 2). This AIE property effectively overcomes aggregation-caused quenching, enabling bright emission in aggregated and solid states. R1 also exhibits ICT emission at 615 nm. Upon Michael addition of HSO_3^- to the C=C bond, the π-conjugation is interrupted and ICT suppressed, resulting in a large ratiometric blue shift (~220 nm) to 396 nm (monomer) and 454 nm (excimer) (Figure 2) [17].

DOI: 10.54254/2753-8818/2026.36819

Su and co-workers [18] reported TPE-YD, a tetraphenylethylene (TPE)-based AIEgen probe combined with an indolium acceptor. Its AIE effect enables strong NIR fluorescence at 710 nm, a large Stokes shift, and high photostability, effectively overcoming aggregation-caused quenching (Figure 2). Michael addition of SO_2 derivatives to the C=C bond disrupted ICT pathway, leading to fluorescence quenching and visible color fading (Figure 2) [18].

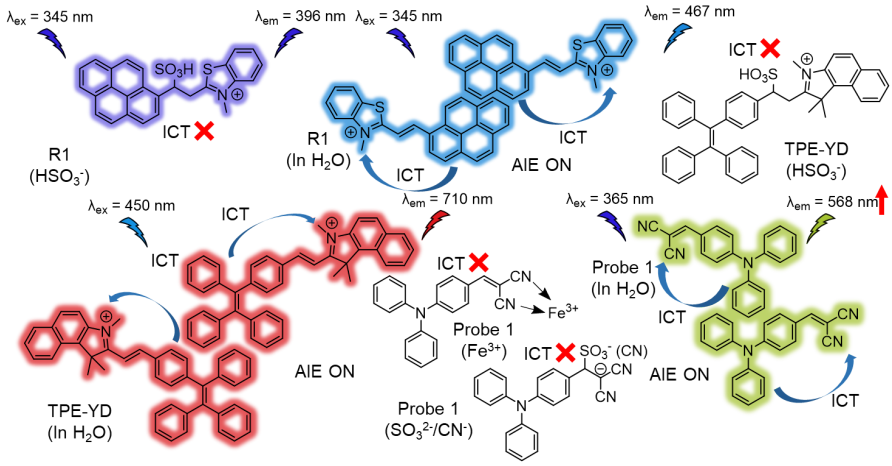

Figure 2. Representative post-reaction structures of Michael addition probes based on AIE [17-19]

In 2015, Yang et al. [19] designed Probe 1, a triphenylamine-based probe incorporating a dicyanovinyl group as the Michael acceptor. Its hydrophobic structure promotes aggregation in aqueous solution, and RIR induces strong AIE fluorescence at 568 nm (Figure 2). Michael addition of SO_3^{2-} to the vinyl group interrupted the π-conjugation, and fluorescence quenching (Figure 2). Similarly, CN^- undergoes nucleophilic addition to the dicyanovinyl double bond, while Fe^{3+} induces a hyperconjugation effect, both leading to ICT suppression (Figure 2) [19].

2.1.3. TICT-modulated probes

Twisted Intramolecular Charge Transfer (TICT) arises in donor-acceptor (D-A) systems when excited-state rotation drives the junction toward a perpendicular geometry [10]. The charge transfer (CT) surface is shaped by competing forces: electron transfer (ET) character favors twisting, whereas locally excited (LE) character stabilizes coplanarity [10]. Strong donors and acceptors stabilize the twisted ET state, while π-π mesomeric interactions lower the LE level and promote planarization [10]. When HSO_3^-/SO_3^{2-} undergoes Michael addition to a C=C bond, the reaction perturbs the electronic structure, drives the TICT process, and quenches fluorescence. Conversely, under certain conditions such as high viscosity, molecular rotation can be structurally restricted, suppressing the TICT process and thereby generating fluorescence [20, 21].

Peng et al. [20] reported ES, a D-π-A structured probe integrating Michael addition, ICT, and TICT processes. The probe consists of a phenol-functionalized thiophene donor and an indole salt acceptor, connected through an alkene double bond. Upon nucleophilic addition of SO_2 to the alkene bond, the ICT pathway is blocked, resulting in fluorescence quenching at 628 nm (Figure 3) [20].

Yang et al. [21] designed CNNP, an "OR" logic gate probe integrating Michael addition and ICT processes. Structurally, CNNP is a D-π-A conjugated carbazole derivative (electron donor) linked to dual-cationic 1,1,2-trimethyl-1H-benzo[e]indole units (electron acceptors). Upon Michael addition of HSO_3^- to the C=C bond, the D-π-A conjugation is disrupted, producing a blue-shifted turn-on fluorescence at 470 nm (Figure 3) [21].

DOI: 10.54254/2753-8818/2026.36819

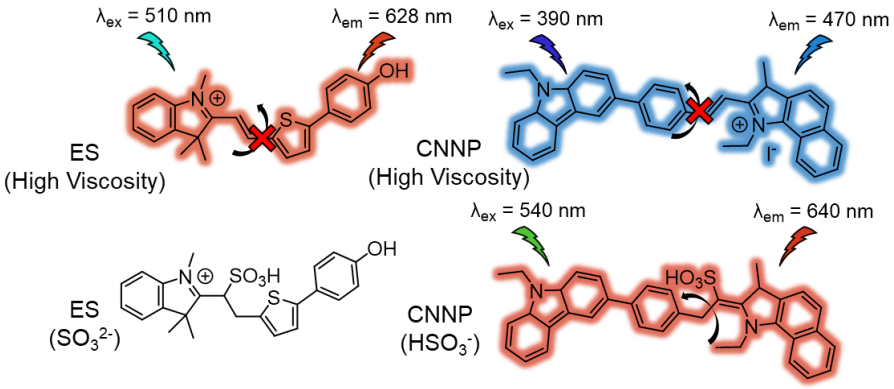

Figure 3. Representative post-reaction structures of Michael addition probes based on TICT [20, 21]

2.1.4. FRET-modulated probe

Förster resonance energy transfer (FRET) is a non-radiative process in which energy from an excited donor is transferred to a ground-state acceptor via dipole-dipole coupling [9, 12]. Efficient FRET requires donor-acceptor spectral overlap within 1-10 nm [9, 12].. In sulfite-responsive FRET probes, nucleophilic addition of HSO_3^-/SO_3^{2-} to the conjugated acceptor disrupts its structure, altering spectral overlap and thereby terminating or restoring FRET. As a result, donor emission may recover or be quenched, while acceptor emission correspondingly decreases or increases. Its ratiometric responses provide accurate sulfite quantification with built-in correction for environmental interference [9, 12].

Dong et al. [22] designed CPP, a coumarin-based ratiometric probe integrating Michael addition chemistry with a FRET mechanism. It consists of a donor, 7-(diethylamino)coumarin-3-amide, and an acceptor, phenyl-2-(pyridine-4-yl)acrylonitrile. Michael addition of HSO_3^- to the acrylonitrile C=C bond, disrupts the acceptor conjugation, suppressing FRET and shifting emission from 605 nm (orange) to 485 nm (blue) (Figure 4) [22].

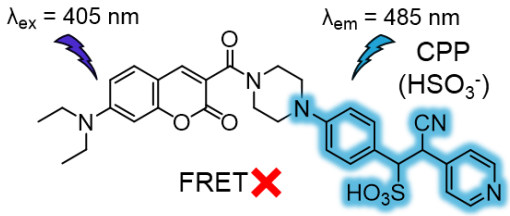

Figure 4. Representative post-reaction structure of Michael addition probe based on FRET [22]

2.1.5. Metal complex probe

Metal complex-based fluorescence probes employ heavy transition-metal complexes (Ir^{3+}, Ru^{2+}, Pt^{2+}) as luminescent units [9]. Their phosphorescence arises from metal-to-ligand (MLCT) or ligand-to-metal (LMCT) charge-transfer states, facilitated by strong spin-orbit coupling. Enhanced intersystem crossing (ISC) efficiently populates the triplet manifold (T_1) state, enabling spin-forbidden radiative decay from T_1 to the singlet ground state (S_0). This process produces long-lived phosphorescence characterized by large Stokes shifts and visible-light excitation (λ_{ex} > 550 nm) [9].

DOI: 10.54254/2753-8818/2026.36819

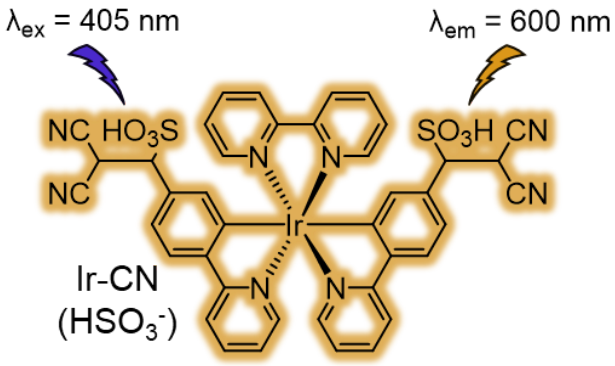

Figure 5. Representative post-reaction structure of metal-complex probe [23]

Xin et al. [23] reported Ir-CN, a cyclometalated iridium(III) complex probe incorporating a dicyanovinyl group as the Michael acceptor. Michael addition of SO_2 derivatives to the C=C bond induces a turn-on phosphorescence at 600 nm (Figure 5) [23].

2.2. Fluorescence probes based aldehyde addition reaction

Aldehyde addition is a nucleophilic reaction in which HSO_3^-/SO_3^{2-} attacks the electrophilic carbon of an aldehyde, forming a stable α-hydroxysulfonate adduct [6]. This consumes the aldehyde moiety altering the conjugation or hydrogen-bonding network of the attached fluorophore. Thus, the fluorescence is modulated, typically appearing as enhancement or ratiometric intensity changes [6].

Dutta and colleagues [24] constructed Kum-C, a β-carboline-based natural product probe containing an aldehyde group as the recognition site. Nucleophilic addition of SO_3^{2-} converts the electron-withdrawing -CHO into -OH, suppressing ICT and producing a turn-on fluorescence at 458 nm (Figure 6) [24].

Excited-state intramolecular proton transfer (ESIPT) is a four-level photocycle (E E* K* K), involving enol (E) and keto (K) phototautomerization [7]. Upon photoexcitation, a proton is rapidly transferred via an intramolecular hydrogen bond, generating a keto tautomer with a large Stokes shift [7, 9]. In sulfite-responsive probes, an aldehyde group serves as the recognition site. Nucleophilic addition of sulfite alters the hydrogen-bonding network suppressing or facilitating the ESIPT. This modulation shifts emission wavelength or intensity, producing turn-on or ratiometric signals with high selectivity [7, 9].

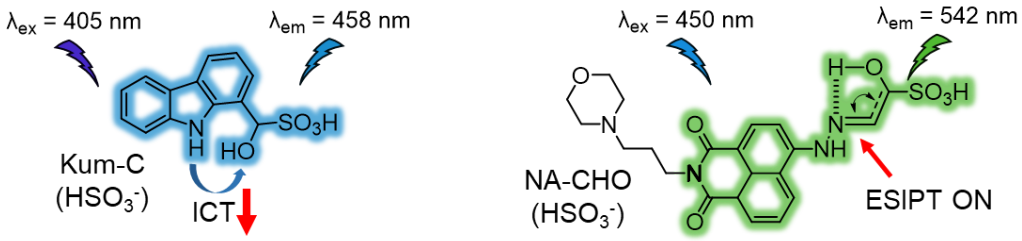

Figure 6. Representative post-reaction structures of aldehyde addition probes [24, 25]

Huo et al. [25] designed NA-CHO, a 1,8-naphthalic anhydride-based probe bearing an aldehyde recognition site. Nucleophilic addition of SO_3^{2-} to the aldehyde, followed by hydrogen-bond-assisted five-membered ring formation, inhibits C=N isomerization and activates the ESIPT pathway, producing a turn-on fluorescence at 542 nm (Figure 6) [25].

DOI: 10.54254/2753-8818/2026.36819

2.3. Levulinate deprotection strategy probes

Levulinate deprotection is a reaction-based strategy in which a levulinoyl ester masks the fluorophore and quenches fluorescence [6]. Nucleophilic addition of HSO_3^-/SO_3^{2-} to the ketone generates an unstable intermediate that rapidly eliminates, releasing the free fluorophore. This restores conjugation and recovers fluorescence [6].

Wang et al. [26] developed YT, a quinoxaline-based probe incorporating a levulinate protecting group to combine deprotection chemistry with ICT modulation. Sulfite-triggered cleavage of the levulinate exposes a hydroxyl group, restoring ICT and producing a green turn-on fluorescence at 466 nm with (Figure 7) [26].

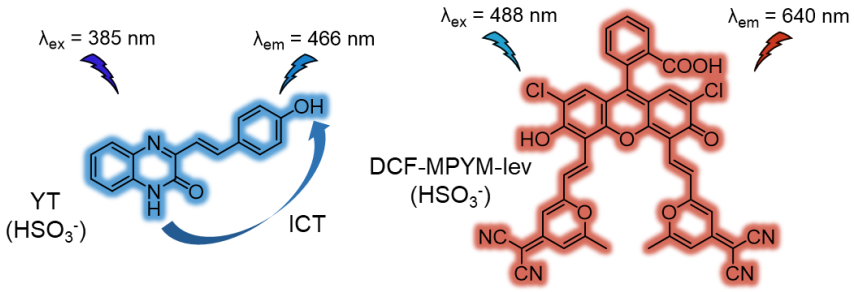

Figure 7. Representative post-reaction structures of levulinate deportation probes [26, 27]

In 2020, Yin et al. [27] developed DCF-MPYM-lev, a fluorescein-based probe incorporating a protecting group that quenches emission. Sulfite cleavage of the levulinate opens the spiro ring to generate DCF-MPYM, restoring fluorescence at 640 nm with a turn-on response (Figure 7) [27].

3. Applications of fluorescence probes

Functional evaluation is an important aspect of fluorescence probe, encompassing both real-sample detection and biological imaging. For real-sample detections, MDQ has been used to quantify sulfite in traditional Chinese medicines and surface water (river, seawater) [15], while MS-Bindol was tested in foods (vermicelli, preserved fruit, wine) [16]. In biological imaging, CPP has been examined for analyzing exogenous and endogenous HSO_3^- in A549 cells and zebrafish [22]. Also, YT's in vivo and in vitro properties have been evaluated in MCF-7/HeLa cells and tumor-bearing mice [26]. In addition, researchers developed on-site detection methods. Dong and coworkers [22] designed paper- and agar-based sensors enabling quantification by smartphone. Su et al. [20] used TPE-YD to quantify sulfite by measuring RGB values under natural light. The evidence demonstrates that fluorescence probes could serve as an alternative approach for sulfite detection across environmental, food, and biological studies.

4. Conclusion

Overall, the classical reaction mechanisms and photophysical processes have been adapted for designing sulfite-responsive probes, as shown in Table 1. Michael addition and aldehyde addition probes generate structural changes and fluorescence signals by nucleophilic addition of sulfite to C=C bonds or aldehyde groups, respectively [6]. While levulinate deprotection probes bear a levulinoyl ester linkage protection group [6]. Their fluorescence emissions are generated by sulfite cleavage the levulinoyl ester, which exposes their fluorescent structures [6].

DOI: 10.54254/2753-8818/2026.36819

The fluorescent structures are designed following photophysical processes, as classified in Table 1. The common processes include D-π-A systems often employed ICT [7-9], D-A systems with rotatable junctions enabling TICT [10], donor-acceptor spectral overlap activating FRET [9, 12], molecular aggregation rise to AIE [11], and excited-state proton transfer enabling ESIPT [7, 9]. Furthermore, heavy transition metals can be incorporated into fluorescent probes to facilitate strong spin-orbit coupling [9]. This yielding triplet-state phosphorescence and large Stokes shifts through ISC form [9].

Table 1. Representative sulfite-responsive fluorescence probes classified by reaction type and photophysical process [13-27]

Mechanisms	Photophysical Processes		Fluorescence Probes	λ_{em} (nm)	Stokes Shift (nm)	Enhance Factors	LOD	Ref
Michael Addition	ICT	Turn-on	DCM-MQE	661	100	100-fold	6 nM	[13]
		Turn-on	DPQ-1	590	100	11-fold	190 nM	[14]
		Turn-on	DPQ-2	600	130	180-fold	3.11 nM	[14]
		NIR Emission	MDQ	670	90		4.16 nM	[15]
		Turn-on	MS-Bindol	490	169	>1000-fold	0.2 nM	[16]
	ICT	Turn-off	ES (for sulfite)	620 (quenching)	110		33.5 nM	[17]
	TICT	Turn-on	ES (for viscosity)	628	118		1.50–312.84 cP	
	TICT	Turn-on	CNNP (for sulfite)	470	80	126-fold	16.64 nM	[18]
		Turn-on	CNNP (for viscosity)	640	100	286-fold		
	AIE	Ratiometric	R1 (For water)	615 (quenching) 467 (enhancing)	122			[19]
	ICT	Ratiometric	R1 (for sulfite)	615 (quenching) 396 (enhancing)	51	19-fold	89 nM (fluorescence) 145 nM (UV-vis)	
	AIE	Turn-on	TPE-YD (for water)	710 (enhancing)	260			[20]
	ICT	Turn-off	TPE-YD (for sulfite)	710 (quenching)			61 nM (fluorescence); 57 nM (colorimetry)	
	AIE	Turn-on	Probe 1 (for water)	568 (enhancing)	203	82% decrease	107 nM (sulfite) 9.88 nM (CN^-) 1.44 nM (Fe^{3+})	[21]

DOI: 10.54254/2753-8818/2026.36819

Table 1. (continued)

	ICT	Turn-off	Probe 1 (avaliable for sulfite, CN^-, Fe^{3+})	568 (quenching)	203	82% decrease	107 nM (sulfite) 9.88 nM (CN^-) 1.44 nM (Fe^{3+})	[21]
	FRET	Ratiometric	CPP	605 (quenching) & 485 (enhancing)	80		3.25 μM	[22]
		Turn-on	Ir-CN (Metal complex)	600	195		0.17 μM	[23]
Aldehyde Addition	ICT	Turn-on	Kum-C	458	53	15-fold	0.35 μM	[24]
	ESIPT	Turn-on	NA-CHO	542	92		330 μM	[25]
Levulinate Deprotection	ICT	Turn-on	YT	466	81	120-fold	0.15 μM	[26]
	TADF	Turn-on	DCF-MPYM-lev	640	152		2.98 μM	[27]

Fluorescence probes provide unique advantages compared with traditional methods. As summarized in Table 2, the applications of probes crossing bioimaging (e.g. cells, mice, zebrafish), quantification of sulfite in real-samples (i.e. foods, water, medicines), and on-site detection (e.g. paper- and agar-based sensors). They usually have rapid response times, such as DCM-MQE response within 3 s [13] and DPQ-1/2 response within 5 s [14]. Moreover, high selectivity of probes implies the quantifying ability under complex condition. For example, Kum-C has demonstrated high selectivity across anions, biothiols, and metal ions [24]. Therefore, the wide applications, rapid response times, high selectivity , and moderate reaction mechanisms achieve the convenience, multi-functional, and various advantages properties of fluorescence probes.

Table 2. Summary of sulfite-responsive fluorescence probes and their verified applications [13-27]

Fluorescence Probes	Response Times	Targets	Applications	Ref.
DCM-MQE	3 s	HeLa Cells	In vitro/vivo application	[13]
DPQ-1	<5 s	Mitochondria	In vitro/vivo applications Real sample analysis Colorimetric kit	[14]
DPQ-2	<5 s			[14]
MDQ	<400 s	Traditional Chinese medicines; Surface water	Portable fluorescence detector for field testing	[15]
MS-Bindol	<90 s	Mitochondria	In vitro/vivo applications Real-sample analysis	[16]

DOI: 10.54254/2753-8818/2026.36819

Table 2. (continued)

ES	<30 s (for sulfite)	Mitochondria	In vitro/vivo applications	[17]
CNNP	<1 min (for sulfite)	Lipid droplet (for sulfite) Mitochondria (for viscosity)	In vitro/vivo applications Real-sample analysis	[18]
R1	1 min (colorimetric) 5 min (fluorometric)	HeLa Cells	In vitro application Colorimetric kit	[19]
TPE-YD	<10 min (for sulfite)	Mitochondria	In vitro applications Real-sample analysis Colorimetric kit	[20]
Probe 1	<30 min (sulfite, CN^-, Fe^{3+})	HeLa Cells	Fe^{3+}: In vitro application Colorimetric kit Sulfite & CN^-:Colorimetric kit	[21]
CPP	<25 min (aquous) 32-36 min (solid-state)	A549 Cells	In vitro/vivo applications Real sample analysis Colorimetric kit	[22]
Ir-CN		Mitochondria	In vitro application	[23]
Kum-C		U2OS Cells	In vitro application Real-sample analysis	[24]
NA-CHO	<30 s	HeLa Cells	In vitro/vivo applications	[25]
YT	<10 min	MCF-7 Hela Cells	In vitro/vivo applications	[26]
DCF-MPYM-lev	<20 min	MCF-7 Cells	In vitro application	[27]

Although fluorescence probes have been demonstrated to be effective for wide application, they still have limitations for imaging in biological models. Long-wavelength emission is required for deep-tissue imaging [28]. Bulky molecular structure or high hydrophobicity may hinder cell uptake, thereby affecting the imaging performance [29, 30]. Furthermore, issues regarding the potential toxicity and adverse reactions of the probes during their administration in living tissues still need to be addressed. Thus, further research should focus on optimizing their physical, photophysical, and biocompatibility properties.

DOI: 10.54254/2753-8818/2026.36819

References

[1] Stauffer, C. B., & Tat, J. (2026). Toxic effects of sulfur dioxide: A review. *Toxics, 14*(1), 100. https://doi.org/10.3390/toxics14010100

[2] Huang, Y., Zhang, H., Lv, B., Tang, C., Du, J., & Jin, H. (2021). Sulfur dioxide: Endogenous generation, biological effects, detection, and therapeutic potential. *Antioxidants and Redox Signaling, 36*(4–6), 256–274. https://doi.org/10.1089/ars.2021.0213

[3] Schwarz, G., & Veldman, A. (2015). Molybdenum cofactor disorders. In J. Blau, M. Duran, & K. M. Gibson (Eds.), *Physician's guide to the diagnosis, treatment, and follow-up of inherited metabolic diseases* (pp. 191–199). Springer.

[4] Schwarz, G. (2016). Molybdenum cofactor and human disease. *Current Opinion in Chemical Biology, 31*, 179–187. https://doi.org/10.1016/j.cbpa.2016.03.016

[5] Pundir, C. S., & Rawal, R. (2013). Determination of sulfite with emphasis on biosensing methods: A review. *Analytical and Bioanalytical Chemistry, 405*(10), 3049–3062. https://doi.org/10.1007/s00216-013-6753-0

[6] Yang, B., Xu, J., & Zhu, H. (2019). Recent progress in the small-molecule fluorescent probes for the detection of sulfur dioxide derivatives (HSO_3^-/SO_3^{2-}). *Free Radical Biology and Medicine, 145*, 42–60. https://doi.org/10.1016/j.freeradbiomed.2019.09.007

[7] Mondal, A., Mondal, P., & Chattopadhyay, P. (2024). Regulatory principles, parameters and probe design to ascertain the interconnection between ICT, ESIPT and PET mechanisms. *Inorganica Chimica Acta, 571*, 122194. https://doi.org/10.1016/j.ica.2024.122194

[8] Li, T., Chen, X., Wang, K., & Hu, Z. (2022). Small-molecule fluorescent probe for detection of sulfite. *Pharmaceuticals, 15*(11), 1326. https://doi.org/10.3390/ph15111326

[9] Liu, Z., He, W., & Guo, Z. (2013). Metal coordination in photoluminescent sensing. *Chemical Society Reviews, 42*(4), 1568. https://doi.org/10.1039/c2cs35363f

[10] Sasaki, S., Drummen, G. P. C., & Konishi, G. (2016). Recent advances in twisted intramolecular charge transfer (TICT) fluorescence and related phenomena in materials chemistry. *Journal of Materials Chemistry C, 4*(14), 2731–2743. https://doi.org/10.1039/c5tc03933a

[11] Wang, W., Liu, Y., Xu, J., Deng, Y., Chen, W., Lin, Y., Tang, B. Z., & Zhang, M. (2025). Harnessing the power of aggregation-induced emission luminogens: From bright probes to theranostic platforms in biomedicine. *Coordination Chemistry Reviews, 552*, 217553. https://doi.org/10.1016/j.ccr.2025.217553

[12] Fatima, M., & Abbas, N. (2025). Expanding horizons in advancements of FRET biosensing technologies. *Biosensors, 15*(7), 452. https://doi.org/10.3390/bios15070452

[13] Luo, S., Xiang, L., Liu, H., Luo, Y., Shi, L., Liu, G., & Yang, S. (2025). A fluorescent probe for sulfur dioxide reveals intracellular reductive stress triggered by natural antioxidants. *Chemical Communications, 62*(1), 272–275. https://doi.org/10.1039/D5CC05915A

[14] Ji, N., Zhan, Y., Lan, T., Zhang, J., & He, W. (2025). Two activatable fluorescent probes for bisulfite detection: Imaging in living cells and zebrafish, analysis in white wine, and a kit for dried fruit testing. *Dyes and Pigments, 245*, 113056. https://doi.org/10.1016/j.dyepig.2025.113056

[15] Yan, F., Cui, J., Wang, C., Tian, X., Li, D., Wang, Y., Zhang, B., Feng, L., Huang, S., & Ma, X. (2022). Real-time quantification for sulfite using a turn-on NIR fluorescent probe equipped with a portable fluorescence detector. *Chinese Chemical Letters, 33*(9), 4219–4222. https://doi.org/10.1016/j.cclet.2022.03.006

[16] Zhang, X., Zhang, L., Zhang, L., Liu, S., Zhu, X., Zhou, P., Cheng, X., Zhang, R., Zhang, L., Zhang, L., & Chen, L. (2021). Insight into sulfur dioxide and its derivatives metabolism in living system with visualized evidences via ultra-sensitive fluorescent probe. *Journal of Hazardous Materials, 423*(Pt B), 127179. https://doi.org/10.1016/j.jhazmat.2021.127179

[17] Diwan, U., Kumar, V., Mishra, R. K., Rana, N. K., Koch, B., Singh, M. K., & Upadhyay, K. (2016). A pyrene-benzothiazolium conjugate portraying aggregation-induced emission, a ratiometric detection and live cell visualization of HSO_3^-. *Analytica Chimica Acta, 929*, 39–48. https://doi.org/10.1016/j.aca.2016.04.057

[18] Su, X., Zeng, R., Huang, X., Lan, J., Li, Z., Yan, Z., Tang, C., Jing, L., Ding, Y., Zhang, T., & Jiang, N. (2025). A versatile aggregation-induced emission probe: Accurate quantification, on-site detection, and bioimaging of sulfur dioxide derivatives using a colorimetric and near-infrared fluorescent probe. *Talanta, 298*(Pt B), 128953. https://doi.org/10.1016/j.talanta.2025.128953

[19] Yang, X., Chen, X., Lu, X., Yan, C., Xu, Y., Hang, X., Qu, J., & Liu, R. (2015). A highly selective and sensitive fluorescent chemosensor for detection of CN^-, SO_3^{2-} and Fe^{3+} based on aggregation-induced emission. *Journal of Materials Chemistry C, 4*(2), 383–390. https://doi.org/10.1039/C5TC02865E

DOI: 10.54254/2753-8818/2026.36819

[20] Peng, Z., Zhang, D., Yang, H., Zhou, Z., Wang, F., Wang, Z., Ren, J., & Wang, E. (2024). Mitochondria-targeted fluorescent probe for simultaneously imaging viscosity and sulfite in inflammation models. *The Analyst, 149*(12), 3356–3362. https://doi.org/10.1039/D4AN00467A

[21] Yang, T., Fang, Y., Ye, K., Wang, C., Wang, F., & Li, C. (2024). A multifunctional fluorescent probe for monitoring of SO_2 and viscosity and its application in food, ferroptosis, and bioimaging. *Sensors and Actuators B: Chemical, 426*, 137024. https://doi.org/10.1016/j.snb.2024.137024

[22] Dong, S., Zhang, Y., Huang, Y., Zhang, Y., Yang, G., Chen, C., Wang, L., Huo, J., Lu, P., & Cao, D. (2025). A FRET ratiometric fluorescent probe for detection of bisulfite in food: Insights into food quality and preservation. *Analytica Chimica Acta, 1373*, 344558. https://doi.org/10.1016/j.aca.2025.344558

[23] Xin, H., Huang, Y., Han, Y., Tang, L., Yang, G., Zhang, Y., Zhao, S., Wang, K., Li, Y., & Cao, D. (2023). A two-photon iridium(III) complex probe for sensitive detection of SO_2 derivatives in living cell mitochondria. *Spectrochimica Acta Part A: Molecular and Biomolecular Spectroscopy, 299*, 122876. https://doi.org/10.1016/j.saa.2023.122876

[24] Dutta, K., Chattaraj, S., Pal, R., Jonnalgadda, P. N., Patro, B. S., Mula, S., & Chakraborty, G. (2024). A Kumujian-C based highly selective fluorescence turn-on probe enables the detection of sulfite in real samples and living cells. *New Journal of Chemistry, 48*(22), 9961–9969. https://doi.org/10.1039/D4NJ01136H

[25] Huo, F., Wu, Q., Yin, C., Zhang, W., & Zhang, Y. (2019). A highly efficient and lysosome-targeted "off–on" probe for sulfite based on nucleophilic addition and ESIPT. *Spectrochimica Acta Part A: Molecular and Biomolecular Spectroscopy, 214*, 429–435. https://doi.org/10.1016/j.saa.2019.02.045

[26] Wang, K., Li, T., Yang, X., Zhang, K., Jiang, Y., Zou, L., Yang, Y., & Hu, Z. (2022). Imaging fluctuation of sulfite in mouse tumor and inflammation models with a novel quinoxaline-based fluorescent probe. *Sensors and Actuators B: Chemical, 365*, 131878. https://doi.org/10.1016/j.snb.2022.131878

[27] Yin, H., Wu, Y., Peng, X., & Song, F. (2020). A turn-on TADF chemosensor for sulfite with a microsecond-scale luminescence lifetime. *Chemical Communications, 56*(72), 10549–10551. https://doi.org/10.1039/D0CC04506C

[28] Wanderi, K., & Cui, Z. (2022). Organic fluorescent nanoprobes with NIR-IIb characteristics for deep learning. *Exploration, 2*(2), 20210097. https://doi.org/10.1002/EXP.20210097

[29] Wender, P. A., Mitchell, D. J., Pattabiraman, K., Pelkey, E. T., Steinman, L., & Rothbard, J. B. (2000). The design, synthesis, and evaluation of molecules that enable or enhance cellular uptake: Peptoid molecular transporters. *Proceedings of the National Academy of Sciences, 97*(24), 13003–13008. https://doi.org/10.1073/pnas.97.24.13003

[30] Zhang, R., Qin, X., Kong, F., Chen, P., & Pan, G. (2019). Improving cellular uptake of therapeutic entities through interaction with components of cell membrane. *Drug Delivery, 26*(1), 328–342. https://doi.org/10.1080/10717544.2019.1582730